ELSEVIER

Catalysis Today 83 (2003) 213–222

CATALYSIS TODAY

www.elsevier.com/locate/cattod

# Preparation of Mn substituted La-hexaaluminate catalysts by using supercritical drying

Junwei Wang, Zhijian Tian*, Jinguang Xu, Yunpeng Xu, Zhusheng Xu, Liwu Lin

*Dalian Institute of Chemical Physics, Chinese Academy of Sciences, Dalian 116023, China*

Received 1 May 2002; received in revised form 23 November 2002; accepted 18 March 2003

**Abstract**

$LaMn_xAl_{12-x}O_{19}$ catalysts were prepared from $NH_4OH$ and metal nitrates solutions. Supercritical drying (SCD) and conventional oven drying (CD) methods were used to extract the water in the hydrogel. The effects of drying methods on properties of the catalysts were investigated by means of TEM, $N_2$-adsorption, thermogravimetry (TG)–differential thermal analysis (DTA) and X-ray diffraction. SCD method is beneficial to maintain high surface area and improving catalytic activity for methane combustion of the catalyst. The specific surface area and pore volume of $LaMn_1Al_{11}O_{19}$ catalyst prepared by SCD method are 28 $m^2$/g and 0.23 $cm^3$/g, respectively, and the ignition of methane could be carried out at 450 °C. However, those of the CD catalyst prepared from the same precursor are 15 $m^2$/g, 0.11 $cm^3$/g and 530 °C, respectively. Suitable Mn content ($0 \leq x \leq 2$) could promote the formation of $LaMnAl_{11}O_{19}$ hexaaluminate, while further addition of Mn ($2 < x \leq 6$) cause the formation of $LaMnO_3$.


*Keywords:* Methane combustion; Hexaaluminate; Supercritical drying; Aerogel; Xerogel

## 1. Introduction

In recent years, high-temperature catalytic combustion of methane has received considerable attention because of the more efficient burning in wider air-to-fuel ratio and with lower $NO_x$ emissions than the conventional thermal combustion. Methane combustion has been proposed for many industrial applications, such as gas turbines, jet engines, etc. In these applications, the operation temperature is in the range of 1000–1400 °C. Therefore, the major difficulty is the development of a practical catalyst that has both high-temperature stability and low-temperature activity [1–4]. Various heat resistant metal oxides have been tested as catalysts and supports for the combustion of methane, such as hexaaluminates, perovskites, spinels, etc. [5–10]. Hexaaluminates related compounds are considered to be one of the most suitable materials for high-temperature catalytic combustion of methane due to their excellent thermal stability and high activity. Most studies so far are focusing on transition metal cations substituted Ba, Sr–La and La-hexaaluminates [5,11–15]. Arai and coworkers [5] first used an alkoxide hydrolysis method to prepare Ba-hexaaluminates catalysts for methane combustion. Groppi et al. [12] reported an $(NH_4)_2CO_3$ coprecipitation method to prepare $BaMnAl_{11}O_{19}$ hexaaluminate and got a comparable result with Arai et al. Then, following the preparation procedure of Groppi et al, Jang et al. [13] prepared a Mn substituted La-hexaaluminate catalyst, over which the $T_{10\%}$ (temperature for 10 vol.% methane conversion) for methane combustion was 450 °C. However, it was found that activity of the

* Corresponding author. Tel./fax: +86-411-4379151.
*E-mail address:* tianz@dicp.ac.cn (Z. Tian).

0920-5861/$ – see front matter © 2003 Elsevier B.V. All rights reserved.
doi:10.1016/S0920-5861(03)00238-4

catalyst prepared by using $NH_4OH$ for coprecipitation was much low. Recently, Zarur et al. [15–17] reported a Ce–Ba-hexaaluminate catalyst prepared by the reverse microemulsion method, and over this catalyst, the $T_{10\%}$ for methane combustion was only about 400 °C. They also investigated the effect of drying methods on the texture of $BaO{\cdot}6Al_2O_3$ hexaaluminate samples, and found that the surface areas of the samples dried by supercritical drying (SCD) method with ethanol were much higher than those by oven drying. The highest surface area of the sample was 136 $m^2/g$ even after calcination at 1300 °C for 2 h, which was about twice of that of the sample dried by oven drying method. For the formation of hydrogels via the sol–gel process, the conventional oven drying (CD) procedure will lead to serious collapse of the structure of hydrogel due to capillary stress caused by the surface tension of water. Under the supercritical state, however, the interface between vapor and liquid will disappear, thus eliminating the surface tension of the liquid. Therefore, if the hydrogel is dried under the supercritical state of a suitable liquid, the capillary stress will be eliminated, and the structure of the hydrogel will be maintained, which is beneficial to reduce the loss of surface area during calcination [17].

The $LaMnAl_{11}O_{19}$ catalyst has been found to possess much higher catalytic activity than Ba–Mn and $Sr_{1-x}$–$La_x$–Mn hexaaluminates catalysts [13]. If the SCD method is used to prepare $LaMnAl_{11}O_{19}$ catalyst, catalytic activity of which might be improved. In this work, SCD method was used to prepare $LaMn_xAl_{12-x}O_{19}$ catalysts. The catalytic activities for methane combustion of the catalysts were investigated. Moreover, TEM, $N_2$-adsorption, thermogravimetry (TG)–differential thermal analysis (DTA) and X-ray diffraction (XRD) were used to study the effects of drying methods as well as Mn content on the properties of the $LaMn_xAl_{12-x}O_{19}$ catalysts.

## 2. Experimental

### 2.1. Preparation of the catalysts

$LaMn_xAl_{12-x}O_{19}$ catalysts were prepared as follows.

First, the mixed appropriate amounts of manganese, lanthanum and aluminum nitrates solution was added into a well-stirred container with an ammonium hydroxide solution at room temperature, while maintaining the pH 9. The mixture solution would then convert to a hydrogel. The hydrogel was aged for 24 h, then filtered, washed with distilled water. The filter cake was divided into two parts. One part was washed by absolute alcohol for three times, then put into a 200 ml autoclave with 100 ml ethanol and kept under supercritical conditions of ethanol (260 °C, 80 atm) for 2 h. Afterwards, the ethanol was slowly released to ambient pressure, and then nitrogen was introduced to purge away the residual ethanol vapor and an aerogel was obtained.

The other part of the cake was put into an oven, dried at 110 °C for 12 h in air, and converted to a xerogel.

Finally, the aerogel and xerogel were calcined in a muffled furnace at 1200 °C for 4 h in air.

### 2.2. Characterization of the catalysts

Specific surface areas and pore structures of the samples were measured on a Micromeritics ASAP 2010 instrument with nitrogen as the adsorption gas.

A transmission electron microscopy (TEM) was performed with a JEOL 200CX electron microscope on the catalysts before and after calcination. TG and DTA were carried out on a Perkin-Elmer Pyris-1 TGA differential thermal analyzer and a DTA-7 thermogravimetric analyzer, respectively.

Crystal structures of the catalysts were determined by a Rigaku DMAX-rB X-ray diffractometer with Cu Kα radiation ($\lambda = 1.542$ Å). The XRD instrument was operated at 40 kV and 50 mA. The spectra were scanned between 5° and 70° ($2\theta$) at a rate of 5°/min.

### 2.3. Catalytic combustion of methane

The reaction of methane combustion was carried out in a conventional flow system under atmospheric pressure. Catalyst (1 ml) (20–40 mesh) was loaded in a quartz reactor (i.d. 10 mm), with quartz beads packed at both ends of the catalyst bed. A mixture gas of methane (1 vol.%) and air (99 vol.%) was fed into the catalyst bed at a gas hourly space velocity of 40 000 $h^{-1}$. The inlet and outlet gas compositions were analyzed by an on-line gas chromatography with a packed column of carbon molecular sieve and a thermal conductivity detector.

## 3. Results and discussions

### 3.1. Effect of drying methods on the properties of $LaMn_1Al_{11}O_{19}$ catalysts

Fig. 1 presents the TEM results of the $LaMn_1Al_{11}O_{19}$ samples. The particle size of xerogel sample is less than 10 nm. The particles of aerogel are fibroid, which are different from that of the xerogel. And the apparent density of aerogel is 0.08 g/cm$^3$, much lower than that of the xerogel (1.3 g/cm$^3$, Table 1). After being calcined at 1200 °C for 4 h, the particle size of CD catalyst derived from xerogel increased and distributed in the range of 60–150 nm. It could be observed that large particles caused by agglomeration of finer particles formed. However, the particle size of SCD catalyst from aerogel increased to 40–80 nm. The range of particle distribution is narrower compared with the CD ones. Table 1 indicates that $S_{BET}$, as well as pore volume and average pore diameter, of the aerogel is much higher than those of the xerogel. After calcination, $S_{BET}$ of SCD catalyst is 28 m$^2$/g, higher than that of the CD one (15 m$^2$/g).

For the hydrogel is formed with much water, so that serious dehydration would happen at elevated temperatures in the oven in air. Simultaneously, collapse and aggregation of hydrogel take place because of the surface tension of water. That leads to the loss of surface areas and the decrease of pore volume of the xerogel. The liquid–gas interface would disappear when the solvent is under the supercritical state [18]. Thereby, the capillary stresses of hydrogel caused by surface tension would be avoided when the hydrogel is dried under the supercritical conditions of ethanol, and the loose skeleton structure of the hydrogel could be maintained. Therefore, the higher surface area, pore volume and pore diameter of the aerogel are obtained.

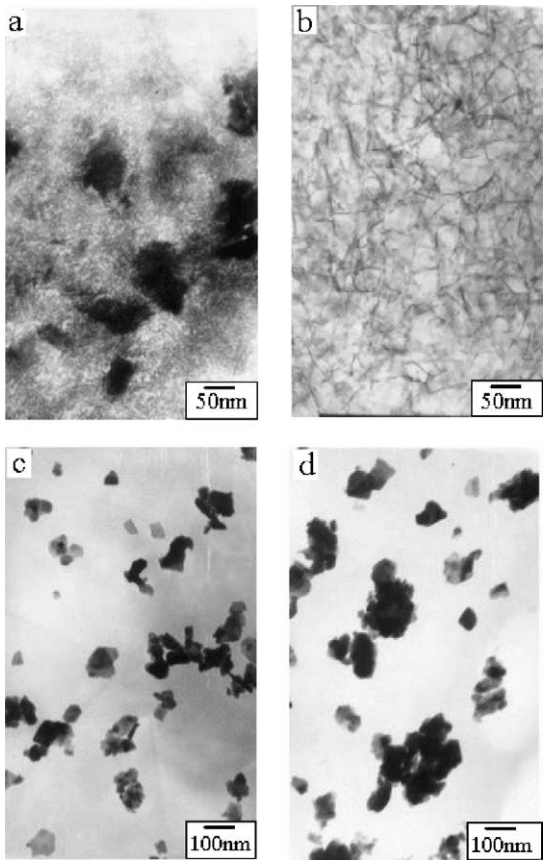


Fig. 1. TEM photographs of $LaMn_1Al_{11}O_{19}$ catalysts before and after calcination: (a) xerogel; (b) aerogel; (c) aerogel derived catalyst; (d) xerogel-derived catalyst.

In addition, average pore diameter of the aerogel is much higher than that of the xerogel. According to Ersson et al., the thermal stability of the sample seems to depend much upon their pore structure. After being heated at 1000 °C, the surface area of the sample found

Table 1
The effect of drying methods on the properties of the $LaMn_1Al_{11}O_{19}$ catalysts[a]

| Drying method | $S_{BET}$ (m$^2$/g) | $V_{pore}$ (cm$^3$/g) | $d_{pore}$ (Å) | $T_{10\%}$ (°C) | $T_{90\%}$ (°C) | Apparent density (g/cm$^3$) |
|---|---|---|---|---|---|---|
| SCD (aerogel) | 360 | 2.40 | 265 | – | – | 0.08 |
| CD (xerogel) | 256 | 0.23 | 35 | – | – | 1.3 |
| SCD | 28 | 0.23 | 324 | 450 | 670 | 0.9 |
| CD | 15 | 0.11 | 281 | 530 | 760 | 1.7 |

[a] $T_{10\%}$, $T_{90\%}$: temperature required for 10 and 90% $CH_4$ conversion, respectively; $V_{pore}$: pore volume; $d_{pore}$: average pore diameter. Reaction conditions: 1% $CH_4$ in air, 40 000 h$^{-1}$ space velocity.

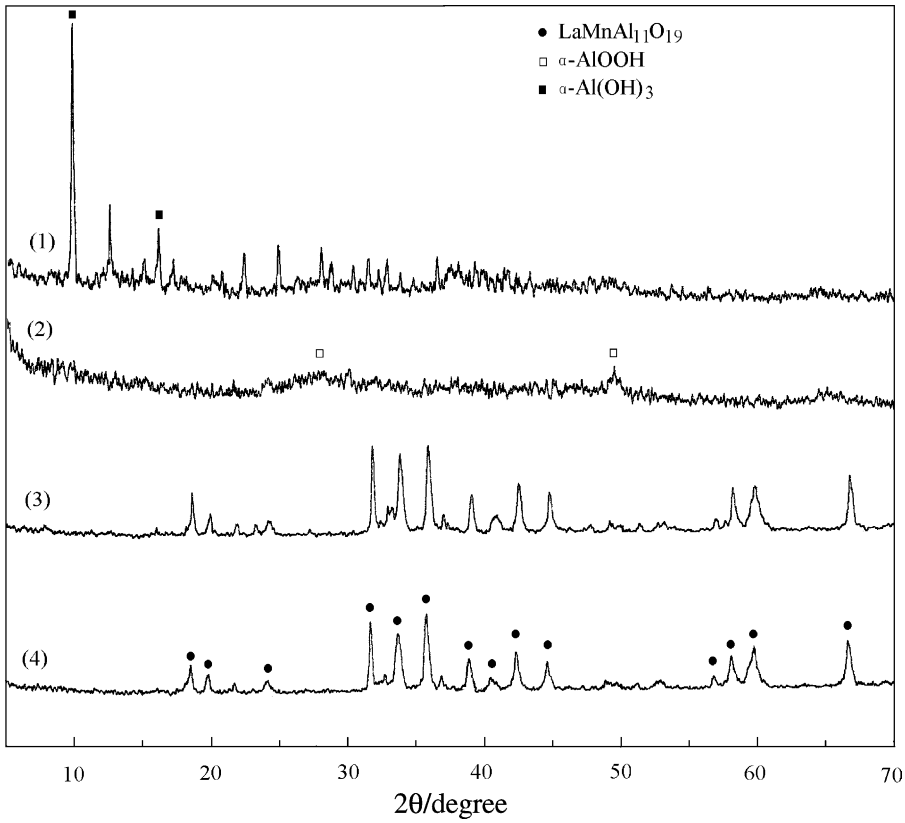


Fig. 2. XRD patterns of $LaMn_1Al_{11}O_{19}$ catalysts before and after calcination: (1) xerogel; (2) aerogel; (3) $LaMn_1Al_{11}O_{19}$ (CD); (4) $LaMn_1Al_{11}O_{19}$ (SCD).

in pores below 50 Å decreased dramatically while the pores above 50 Å survived to a much greater extent and thereby preserved the surface area [19]. The average pore diameter of aerogel and xerogel are 265 and 35 Å, respectively, so that larger surface area of aerogel could be maintained compared with xerogel after being calcined at 1200 °C for 4 h.

XRD patterns in Fig. 2 indicate that aerogel of $LaMn_1Al_{11}O_{19}$ belong to α-AlOOH boehmite. The diffraction peaks of La and Mn hydroxides or oxides could not be found. That means La and Mn species were highly dispersed in the aerogel. It might be related to the preparation method. Since a large amount of water in the hydrogel had been substituted by ethanol during the washing stage, the dehydration of the hydrogel was alleviated, and the migration of La and Mn species from the inner to the surface was restrained. Hence, the homogeneity of the sample could be maintained. The XRD pattern of xerogel $LaMn_1Al_{11}O_{19}$ is complicated. The α-$Al(OH)_3$ and other unknown hydroxides or oxides of La, Mn and Al species appeared. It indicates that La and Mn cations were segregated from xerogel following the vaporization of water when the hydrogel was dried in oven. Compared with aerogel, the homogeneity of the xerogel was destroyed. As a result, the formation temperature of hexaaluminate increased. [20]. After calcination, both samples transformed into hexaaluminate accompanied with a little of $LaAlO_3$, while the intensity of diffraction peaks of aerogel-derived SCD catalyst is weaker and wider than that of the xerogel-derived CD catalyst. Arai and coworkers [11] believed that the crystal growth of hexaaluminate along the *c*-axis is strongly suppressed compared to that along the direction normal to the axis at elevated temperatures. Therefore, if the hexaaluminate formed

with small crystal size, the further growth of crystal would be suppressed and the high surface area would be maintained. The weaker and wider diffraction peaks of SCD catalysts mean that the crystal size is smaller than that of the CD catalysts. TEM photographs also showed the smaller particle size of the SCD catalyst. White suggested that the porous structure could hamper the crystallite growth on grain boundaries and suppress sintering of the sample at high temperatures [21]. So, SCD method provides the aerogel with high pore volumes and large pore diameters, which are beneficial to the formation of

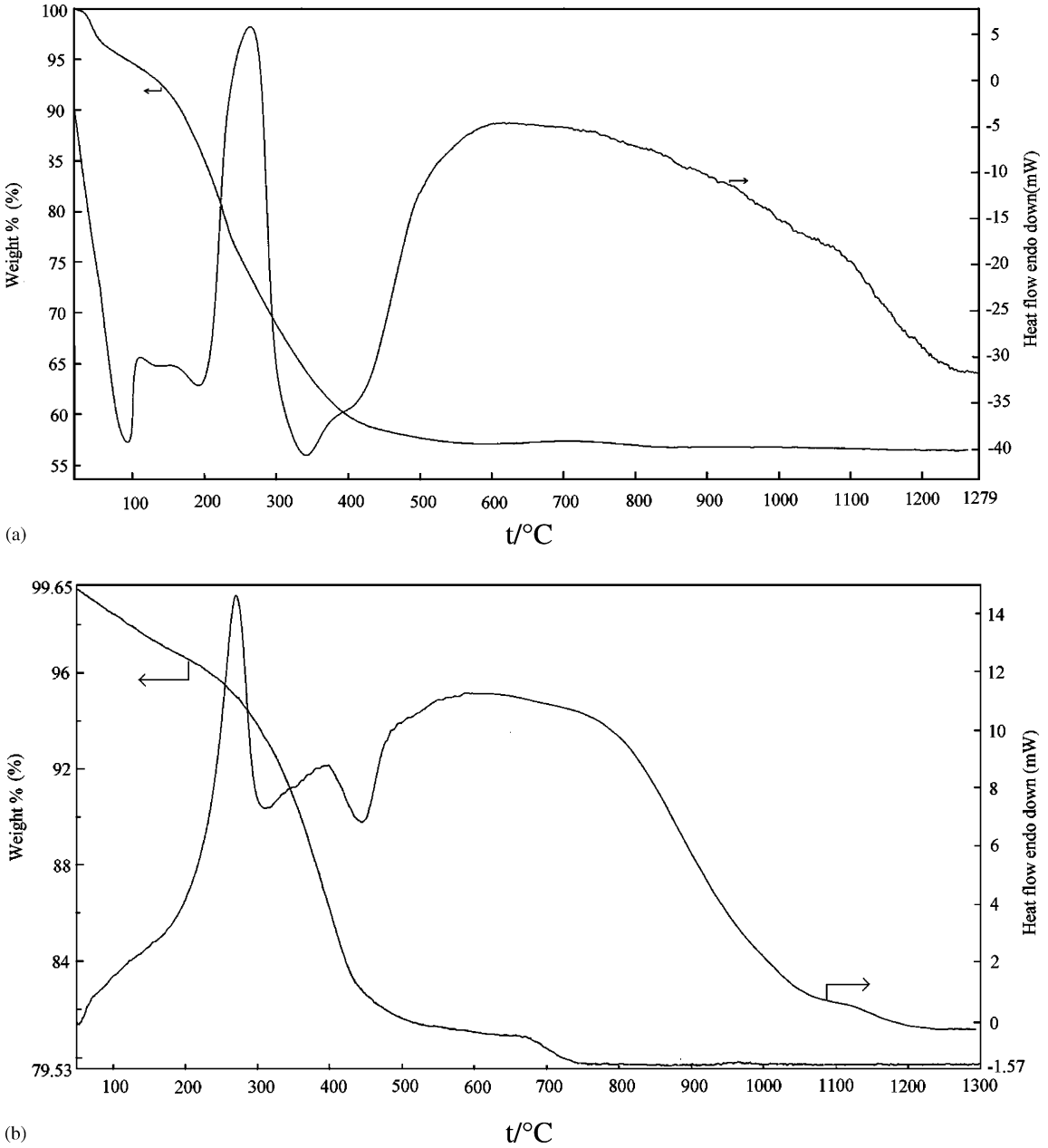


Fig. 3. TG–DTA curves of $LaMn_1Al_{11}O_{19}$ samples: (a) xerogel; (b) aerogel.

hexaaluminate catalyst with fine particles and high surface area.

TG–DTA results are shown in Fig. 3. When the samples were heated from room temperature to 1300 °C, the aerogel and xerogel loses about 20 and 45% of weight, respectively. The weight loss of both samples cannot be observed above 800 °C. DTA curves present three main endothermic peaks of the xerogel in the range of room temperature to 600 °C. During these endothermic stages, the weight loss of the sample was about 5, 20 and 20%, respectively. The peak below 100 °C corresponds to the loss of physically adsorbed water. Both peaks between 100 and 600 °C are caused by the dehydration of the xerogel. Moreover, a weak exothermic peak appears at about 1100 °C. For the aerogel, the exothermic peak appeared between 200 and 300 °C is caused by the oxidation of adsorbed ethanol during the SCD process. In addition, a weak shoulder exothermic peak appeared at 1150 °C.

TG results indicate that the xerogel loses much more weight than aerogel. It means that less dehydroxylations of alumina happened when aerogel converted to hexaaluminate than xerogel during calcination. Thus the sintering and transformation to a transition alumina caused by dehydroxylation could be reduced. For the weak exothermic peak in DTA, it could not be derived from decomposition of the sample because no weight loss was observed at the same temperature in TG curve. XRD result in Fig. 4 also shows that the hexaaluminate was formed from aerogel between 800 and 1000 °C. Therefore, the exothermic peak is related to the transformation of metal oxides into hexaaluminate. The peak of aerogel is about 50 °C higher than that of the xerogel. It means that the transformation of aerogel to hexaaluminate is delayed compared to xerogel. That might be caused by the large pore diameter and high pore volume of aerogel, which limited the interaction of La, Mn and Al species.

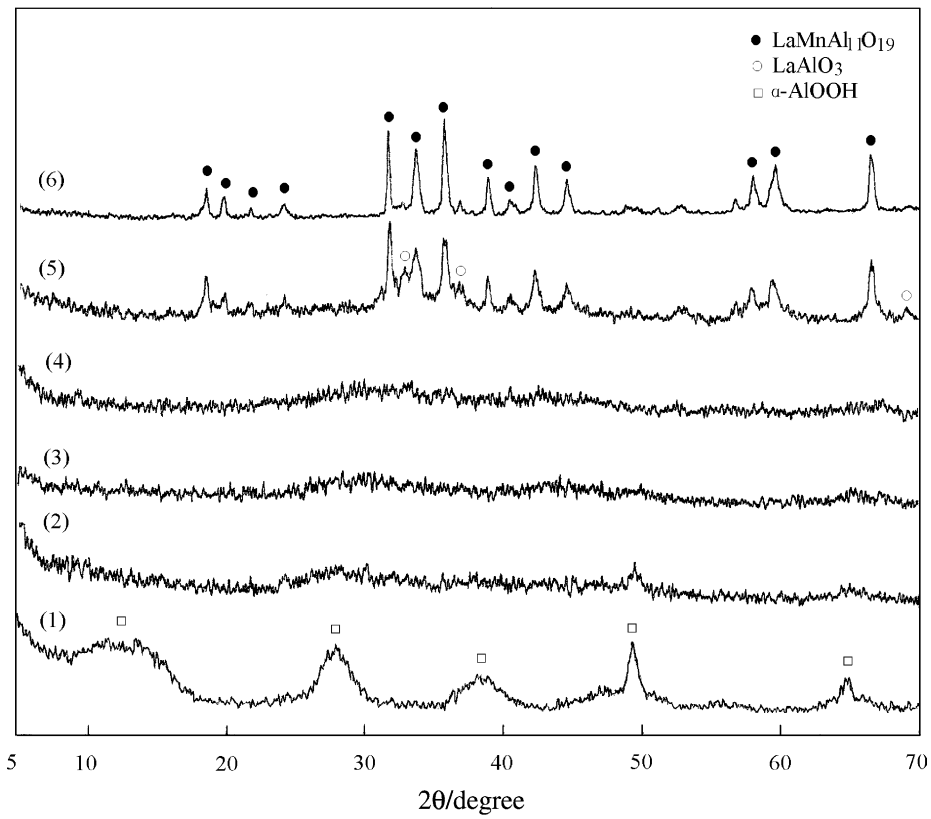


Fig. 4. Effect of calcination temperature on crystal structure of $LaMn_1Al_{11}O_{19}$ (SCD) catalyst: (1) aerogel $Al_2O_3$; (2) aerogel $LaMn_1Al_{11}O_{19}$; (3) 400 °C; (4) 800 °C; (5) 1000 °C; (6) 1200 °C.

The catalytic activities for methane combustion of the catalysts, represented by the temperatures required for 10 and 90 vol.% $CH_4$ conversion ($T_{10\%}$ and $T_{90\%}$), are shown in Table 1. $T_{10\%}$ of the $LaMn_1Al_{11}O_{19}$ (SCD) catalyst is 450 °C, about 80 °C lower than that of the CD catalyst, and $T_{90\%}$ is 90 °C lower. Therefore, the oxidation of methane could be performed more easily over SCD catalyst. The SCD method improves the surface area and pore volume of the catalyst, and promotes the combustion of methane more effectively.

### 3.2. Effect of calcination temperature and time on properties of $LaMn_1Al_{11}O_{19}$

The XRD patterns of $LaMn_1Al_{11}O_{19}$ aerogel calcined at different temperatures are shown in Fig. 4. The aerogel $Al_2O_3$ showed broad diffraction peaks of α-AlOOH. These peaks were weakened when La and Mn hydroxides were introduced. After being calcined at 400 °C for 4 h, the peaks of α-AlOOH disappeared. It means that the sample was converted to amorphous phase or microcrystals. The weak and broad diffraction peaks of $LaMnAl_{11}O_{19}$ hexaaluminate appeared together with a small amount of $LaAlO_3$ at 1000 °C. When the temperature was increased to 1200 °C, the peaks of $LaMnAl_{11}O_{19}$ were strengthened while those of $LaAlO_3$ were weakened. No phase transformation or phase separation occurred even when the sample was calcined at 1250 °C for 10 h, indicating that the catalyst was thermally stable.

For unsubstituted La–Al oxide compounds, Oudet et al. suggested that the introduction of lanthanum to $Al_2O_3$ leads to the nucleation of a cubic $LaAlO_3$ structure on the surface of alumina. Such a surface layer inhibits the surface diffusion or nucleation of transition alumina in the initial step of the phase transformation [22]. Beguin et al. believed that the formation of the $LaAl_{11}O_{19}$ hexaaluminate was associated with a solid-state reaction between δ-$Al_2O_3$ and $LaAlO_3$. Since $LaAlO_3$ is formed from δ-$Al_2O_3$ at 1050 °C [23], the formation of $LaAl_{11}O_{19}$ hexaaluminate should occur at a higher temperature. However,

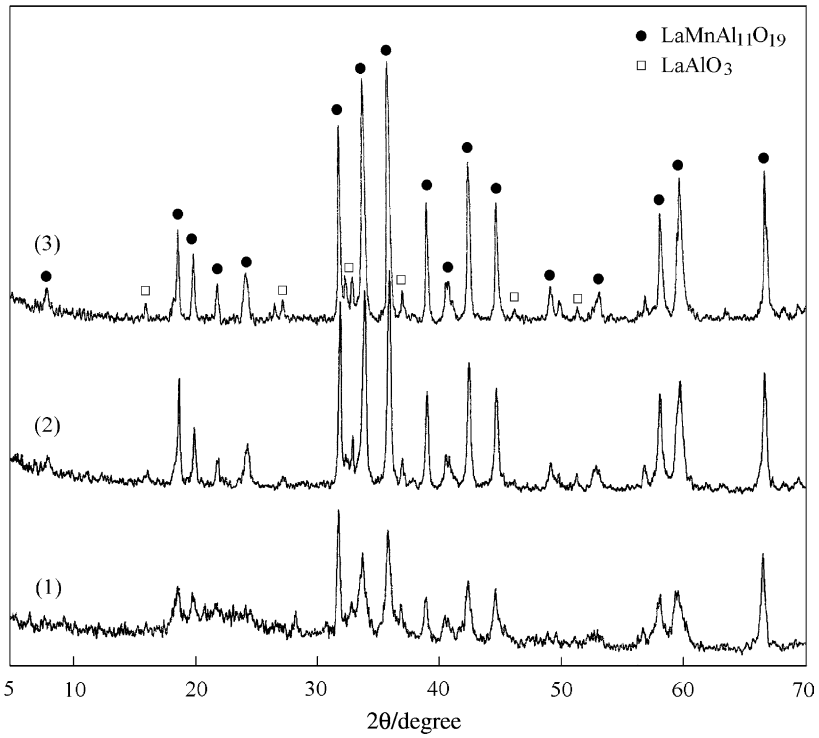


Fig. 5. Effect of calcination time on crystal phase of $LaMnAl_{11}O_{19}$ catalyst. (1) and (2) were calcined at 1200 °C. (1) 2 h; (2) 4 h; (3) 10 h (1250 °C).

the Mn substituted La-hexaaluminate was formed with a little of $LaAlO_3$ at 1000 °C, which indicates that the introduction of Mn oxides promotes the formation of $LaMnAl_{11}O_{19}$ hexaaluminate. In addition, the mechanism of the formation of $LaMnAl_{11}O_{19}$ hexaaluminate might be different from that of $LaAl_{11}O_{19}$. The XRD patterns show that the sample is mainly composed of hexaaluminate at high temperatures. However, $LaAlO_3$ was never found to be the main phase of the sample calcined at different temperatures. It seems that almost all of the La, Mn, and Al oxides converted to hexaaluminate directly from amorphous phase or microcrystal during calcination. Only a little of hexaaluminate was formed via the formation of $LaAlO_3$ as Beguin [23] suggested. Yan and Thompson [24] also reported that Mn substituted $BaO{\cdot}6Al_2O_3$ was converted to hexaaluminate from an amorphous phase directly.

Figs. 5 and 6 present the effects of calcination time on the surface area and crystal structure of the $LaMn_1Al_{11}O_{19}$ (SCD) catalyst at 1200 °C. The surface area decreased with prolonged calcination time. During the first 6 h, the area decreased from 46 to 26 $m^2$/g. After calcined for 10 h, the rate of decrease in surface area became slow. XRD patterns also indicated that the further growth of crystalline hexaaluminate phase was greatly suppressed.

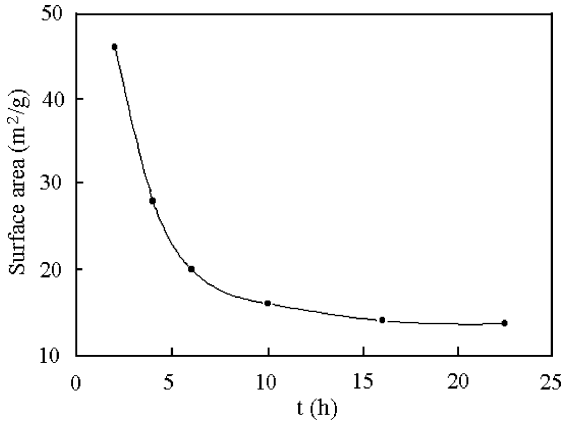


Fig. 6. Effect of calcination time on $S_{BET}$ of $LaMn_1Al_{11}O_{19}$ catalyst.

### 3.3. Effect of Mn content on the properties of $LaMn_xAl_{12-x}O_{19}$ catalysts

In many catalysts, manganese oxides are active phases for methane combustion [2]. Introduction of Mn to $BaO{\cdot}6Al_2O_3$ could also promote the formation of Ba-hexaaluminate at lower temperatures [14], while the Mn content has a threshold for maintaining Ba-hexaaluminate phase [25]. In this work, the effect of Mn loading on morphology and crystal structure of the $LaMn_xAl_{12-x}O_{19}$ catalysts ($0 \leq x \leq 6$) was investigated.

$N_2$-adsorption results are shown in Table 2. The surface area and pore volume decrease with increasing $x$. XRD measurements (Fig. 7) evidenced that the $LaAl_{12}O_{19}$ catalyst was composed of La-hexaaluminate and $LaAlO_3$ perovskite. The weak and broad diffraction peaks implied that the grains were very fine. With the increase of Mn loading in the range of $0 < x < 3$, the diffraction peaks of hexaaluminate were strengthened while those of $LaAlO_3$ perovskite were weakened. However, the further introduction of Mn oxides led to the decrease in the peak intensity of La-hexaaluminate. Moreover, $LaMnO_3$ perovskite appeared. When $x$ was raised to 6, $LaMnO_3$ became the main phase with a little of $MnO_2$.

Table 2
The texture and activity of $LaMn_xAl_{12-x}O_{19}$ catalysts[a]

| $x$ | $S_{BET}$ ($m^2$/g) | $V_{pore}$ ($cm^3$/g) | $d_{pore}$ (Å) | $T_{10\%}$ (°C) | $T_{90\%}$ (°C) | Crystalline phase |
|---|---|---|---|---|---|---|
| 0 | 49 | 0.37 | 293 | 620 | 810 | $LaAlO_3 + LaAl_{11}O_{19}$ |
| 0.5 | 43 | 0.33 | 304 | 515 | 710 | $LaMnAl_{11}O_{19} + LaAlO_3$ |
| 1 | 28 | 0.23 | 324 | 450 | 670 | $LaMnAl_{11}O_{19}$ |
| 2 | 20 | 0.19 | 351 | 450 | 680 | $LaMnAl_{11}O_{19}$ |
| 3 | 15 | 0.15 | 393 | 440 | 700 | $LaMnAl_{11}O_{19} + LaMnO_3$ |
| 6 | 7 | 0.05 | 202 | 450 | 720 | $LaMnO_3 + LaMnAl_{11}O_{19}$ |

[a] All catalysts were calcined at 1200 °C for 4h; $T_{10\%}$, $T_{90\%}$: temperature required for 10 and 90% $CH_4$ conversion, respectively; $V_p$: pore volume; $d_p$: average pore diameter. Reaction conditions: 1% $CH_4$ in air, 40 000 $h^{-1}$ space velocity.

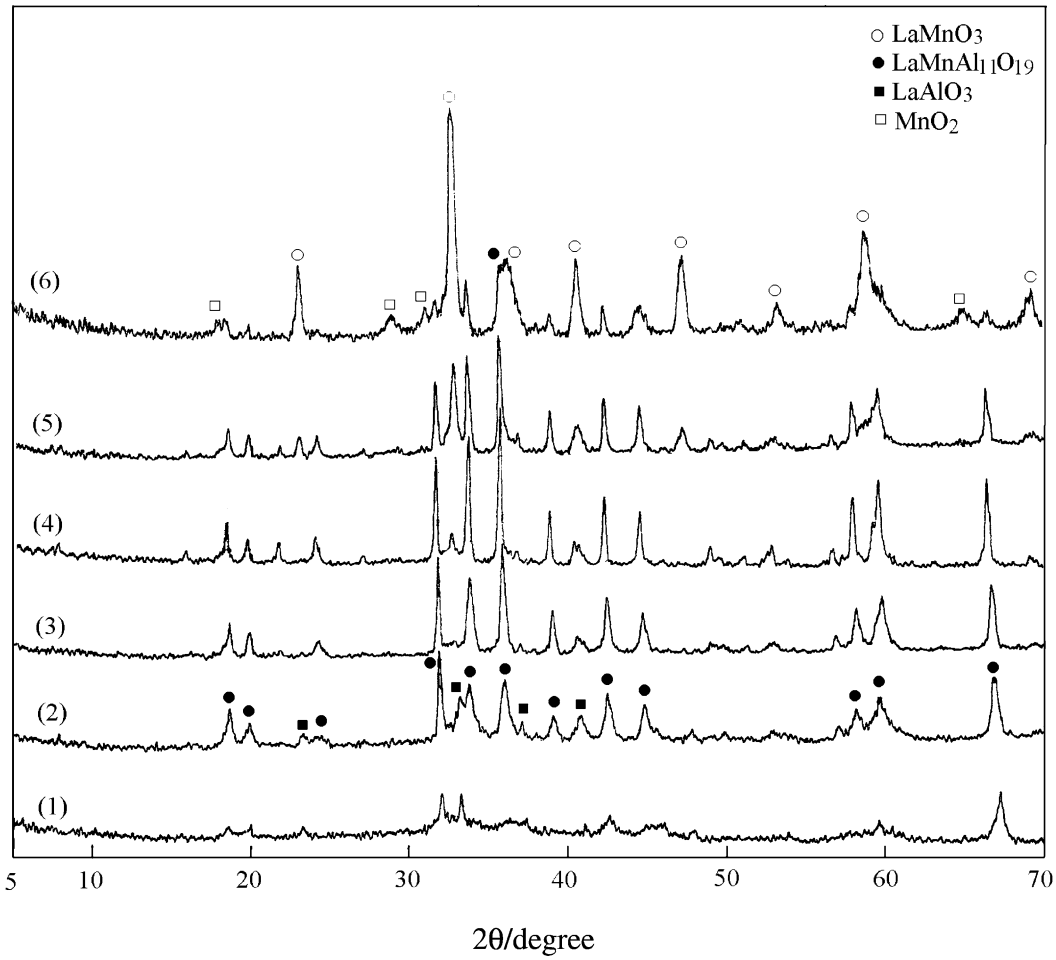


Fig. 7. Effect of Mn content on crystal structure of $LaMn_xAl_{12-x}O_{19}$ catalysts: (1) $x = 0$; (2) $x = 0.5$; (3) $x = 1$; (4) $x = 2$; (5) $x = 3$; (6) $x = 6$.

From the decrease in surface area and pore volume with Mn loading, it seems that Mn could accelerate the sintering of micropores and the agglomeration of fine particles, which led to the decrease in surface area. According to Stobbe et al. [26], the most common manganese oxide phase would assume several oxidation states in air at different temperatures. During calcination, $MnO_2$ would decompose to oxygen and lower valance state manganese oxides, such as $Mn_2O_3$, $Mn_3O_4$ and MnO. In addition, manganese cations, with a smaller diameter than $Al^{3+}$, could enter the lattice of hexaaluminate and occupy the sites of $Al^{3+}$ [25]. Alumina has some defects on the surface, and the surface defects will become very mobile and reactive at a high enough temperature [23]. Although the introduction of lanthanum could prevent alumina from severe sintering, the substitution of the $Al^{3+}$ sites with low charge manganese cations would promote the formation of anion cavities. And then, the $Al^{3+}$ cations near a cavity would migrate close to it in order to maintain the charge balance [25]. Thereby, we thought that the change of valance state of the manganese could promote the migration of $Al^{3+}$, which would cause the agglomeration of $Al_2O_3$ and lead to the decrease of surface area and pore volume. In addition, the migration of $Al^{3+}$ might strengthen the interaction between Al and La, and promote the transformation of $LaMnAl_{11}O_{19}$ hexaaluminate [27].

Since the bond length of Mn–O is longer than that of Al–O, the bond energy of Mn–O is weaker too. If the Mn loading exceeds the threshold, more Mn cations would occupy the $Al^{3+}$ sites, and the structure of hexaaluminate would be destroyed. With further increasing of the Mn content, more La and Mn oxides were converted to $LaMnO_3$ perovskite as shown in Fig. 5. Therefore, a suitable Mn content is very important to maintain the structure and activity of the hexaaluminate catalyst.

The catalytic activities for methane combustion over different $LaMn_xAl_{12-x}O_{19}$ catalysts were shown in Table 2. The initial temperature of methane combustion over $LaAl_{12}O_{19}$ catalyst was decreased obviously after the introduction of Mn oxides. $T_{10\%}$ was 450 °C for the $LaMn_1Al_{11}O_{19}$ catalyst. There is only a slight variation in $T_{10\%}$ for the increase in Mn content from $x = 1$ to 6, while $T_{90\%}$, as an index of complete conversion of methane, increases from 670 to 720 °C. We assume that more Mn oxides introduced could counteract the disadvantageous effect caused by the decrease of surface area of the catalysts with increased oxidation activity of Mn loading. Thus the ignition temperature of methane over $LaMn_xAl_{12-x}O_{19}$ ($1 < x \leq 6$) is close to that of $LaMn_1Al_{11}O_{19}$. However, at high conversions of methane, methane oxidation usually includes surface catalytic reactions and free radical reactions [28]. The free radical reactions depend much more on mass transfer than the catalytic oxidation reaction. Therefore, low surface area would limit the mass transfer of the reactants and cause the $T_{90\%}$ to be elevated.

## 4. Conclusion

The SCD method could prepare homogeneous $LaMn_xAl_{12-x}O_{19}$ aerogel with high pore volumes and pore diameters, which is beneficial to the preparation of catalyst with smaller crystal sizes and higher surface areas than the CD method. Introduction of Mn oxides could greatly enhance the catalytic activity of $LaAl_{12}O_{19}$ catalyst for methane combustion. Mn oxides could promote the formation of $LaMnAl_{11}O_{19}$ hexaaluminate in the range of $0 < x < 3$. A suitable Mn loading is beneficial to methane combustion.

## Acknowledgements

We acknowledge the financial support from Ministry of Science and Technology of the People's Republic of China (G1999022401).

## References

[1] L.D. Pfefferle, W.C. Pfefferle, Catal. Rev.-Sci. Eng. 29 (1987) 219.
[2] M.F.M. Zwinkels, S.G. Järås, P.G. Menon, Catal. Rev.-Sci. Eng. 35 (1993) 319.
[3] D.L. Trimm, Appl. Catal. 7 (1983) 249.
[4] H. Arai, H. Fukuzawa, Catal. Today 26 (1995) 217.
[5] M. Machida, K. Eguchi, H. Arai, Chem. Lett. (1986) 151.
[6] M. Machida, K. Eguchi, H. Arai, J. Catal. 103 (1987) 385.
[7] J.G. McCarty, H. Wise, Catal. Today 8 (1990) 231.
[8] N. Yamazoe, Y. Teraoka, Catal. Today 8 (1990) 175.
[9] Y.F. Yu Yao, J.T. Kummer, J. Catal. 46 (1977) 388.
[10] F. Zamar, A. Trovarelli, C. de Leitenburg, G. Dolcetti, J. Chem. Soc., Chem. Commun. (1995) 965.
[11] M. Machida, K. Eguchi, H. Arai, J. Catal. 123 (1990) 477.
[12] G. Groppi, M. Bellotto, C. Cristiani, P. Forzatti, P.L. Villa, Appl. Catal. A 104 (1993) 101.
[13] B.W.L. Jang, R.M. Nelson, J.J. Spivey, M. Ocal, R. Oukaci, G. Marcelin, Catal. Today 47 (1999) 103.
[14] L. Lietti, C. Cristiani, G. Groppi, P. Forzatti, Catal. Today 59 (2000) 191.
[15] A.J. Zarur, J.Y. Ying, Nature 403 (2000) 65.
[16] A.J. Zarur, H.H. Hwu, J.Y. Ying, Langmuir 16 (2000) 3042.
[17] A.J. Zarur, N.Z. Mehenti, A.T. Heibel, J.Y. Ying, Langmuir 16 (2000) 9168.
[18] Y. Mizushima, M. Hori, J. Mater. Res. 10 (1995) 1424.
[19] A.G. Ersson, E.M. Johansson, S.G. Järås, Stud. Surf. Sci. Catal. 118 (1998) 118.
[20] M. Machida, K. Eguchi, H. Arai, Bull. Chem. Soc. Jpn. 61 (1988) 3659.
[21] J. White, The sintering of industrial powders, in: G.C. Kuczynski (Ed.), Sintering Processes, Plenum Press, New York, 1980, p. 377.
[22] F. Oudet, P. Courtine, A. Vejux, J. Catal. 114 (1988) 112.
[23] B. Beguin, E. Garbowski, M. Primet, Appl. Catal. 75 (1991) 119.
[24] L.C. Yan, L.T. Thompson, Appl. Catal. A 171 (1998) 219.
[25] M. Machida, K. Eguchi, H. Arai, J. Catal. 120 (1989) 377.
[26] E.R. Stobbe, B.A. Boer, J.W. Genus, Catal. Today 47 (1999) 161.
[27] E.M. Johanson, K.M.J. Danielsson, E. Pocoroba, E.D. Haralson, S.G. Järås, Appl. Catal. A 182 (1999) 199.
[28] B.K. Harrison, W.R. Ernst, Combust. Sci. Technol. 19 (1978) 31.